TITLE:

An Analysis of the Stable Cross Section of a Stream Channel

AUTHOR(S):

IWAGAKI, Yuichi; TSUCHIYA, Yoshito

CITATION:

IWAGAKI, Yuichi ...[et al]. An Analysis of the Stable Cross Section of a Stream Channel. Bulletins - Disaster Prevention Research Institute, Kyoto University 1959, 29: 1-27

ISSUE DATE:

1959-03-25

URL:

http://hdl.handle.net/2433/123685

RIGHT:

京都大学学術情報リポジトリ
KURENAI 紅
Kyoto University Research Information Repository

DISASTER PREVENTION RESEARCH INSTITUTE
BULLETIN No. 29 MARCH, 1959

AN ANALYSIS OF THE STABLE CROSS SECTION OF A STREAM CHANNEL

BY

YUICHI IWAGAKI
AND
YOSHITO TSUCHIYA

KYOTO UNIVERSITY, KYOTO, JAPAN

DISASTER PREVENTION RESEARCH INSTITUTE
KYOTO UNIVERSITY
BULLETINS

Bulletin No. 29 March, 1959

An Analysis of the Stable Cross Section of a Stream Channel

By

Yuichi IWAGAKI* and Yoshito TSUCHIYA**

Contents

* Assistant Professor, Disaster Prevention Research Institute, Kyoto University, Japan
** Instructor, Department of Civil Engineering, Nagoya Institute of Technology, Japan

Synopsis

This paper presents an analytical approach to the stable cross section of a stream channel with sand gravels based on the idea of critical tractive force. In this analysis, the two-dimensional flow is assumed to obtain the distribution of shear velocity on the bottom along the cross section of a channel and to apply the turbulence theory to this approach. The theoretical shear distributions computed under such an assumption are verified by the experiment on the velocity-profile measurements by which the shear velocity can be indirectly obtained.

Some fundamental data are presented, which will contribute to design of the stable cross sections of stream channels.

In addition to these theoretical considerations, results of the theoretical analysis are applied to the field data of the existing irrigation canals in the United States of America and India.

1. Introduction

A natural stream channel with erodible material transports usually the sediment load, and gradually the stable condition of the stream channel for both cross section and longitudinal profile is reached at the equilibrium state between the hydraulic characters of stream flow and the sediments constituting the stream channel.

Although the hydraulic treatments of such a stable, sediment-bearing canal are necessary for irrigation and river projects, it is difficult to analyze this problem theoretically due to the very complicated phenomena associated with sediment-transport mechanics and three-dimensional turbulent flow. For practical problems to design canals and channels with erodible material, however, the researches on the stable channel are so fruitful as shown in the references[1),2),3),4),5),6)]. It is especially noted refering to the present paper that, in 1953, Carter, Carlson and Lane[1)] and Lane and Carlson[2)], investigated the effect of the angle of the sloping side on critical tractive force as a fundamental consideration of a stable cross section.

On the other hand, the hydraulic treatment on the mechanics of critical tractive force was first made by Shields[7)] in 1936, and after that, White[8)] and Kurihara[9)] also studied theoretical side of this subject considering the effect

of turbulence. Recently, in 1956, Iwagaki[10], and Iwagaki and Tsuchiya[11] fairly analyzed the mechanics of incipient motion of sand grains in turbulent stream by using the theory of turbulent flow.

In this paper, the stable cross section of a stream channel with non-cohesive material is analyzed in the light of the theory on critical tractive force by Iwagaki[10], based on the concept that all sand grains on the bottom of a channel are under the critical condition for movement. For this approach, it is assumed for simplicity that the stream flow close to sand grains on the bed of the channel can be treated as two-dimensional flow. To verify this assumption, velocity profiles are measured for the flow in the open channels having stable cross sections obtained theoretically and fixed rough beds, and the shear velocity distributions on the bed derived from the measured velocity profiles are compared with the theoretical results. Based on the theoretical stable cross sections, some basic relationships between hydraulic characters and sediment size are presented for practical purpose. Moreover, results of the theoretical analysis are applied to the field data of the irrigation canals which were taken by Simons and Bender[6] and Bureau of Reclamation in the United States of America and taken in India.

2. Hydraulic Treatment of the Stable Cross Section

In analyzing hydraulically the stable cross section based on the concept that all sand grains on the bottom of a channel are under the critical condition for movement, there are two different treatments as the method of approach; the first one is based on the idea that each sand grain bears the shearing force acting on the botton per exposed area of a sand grain as White and Kurihara treated, and the second, a sand grain on the bottom bears the fluid resistance acting on it and the resistance resulting from pressure gradient, which was developed by the authors. The present paper treats this problem by means of the procedure based on the latter idea.

Strictly speaking, any flow in an open channel is three dimensional and no such study on turbulent flow was touched up to now. However, as is seen in the next chapter, it is fairly sufficient with the aid of experimentation that the flow close to sand grains on the bottom of the channel is two-dimensionally treated for each section on the stable channel obtained by the approach of this paper. In deriving the equation expressing the stable cross

section, therefore, the flow near to sand grains is assumed to be locally two-dimensional flow, especially in the case of calculating the pressure gradient resulting from velocity fluctuation. Besides this assumption, the coordinate for the velocity profile will be taken in the normal direction to the bottom of the channel in order to apply the concept of mixing length in the momentum transfer theory by Prandtl.

2.1 Equation of the stable cross section of a stream channel

Now consider the hydraulic condition for the beginning of motion of a spherical sand grain on a section of the channel bottom, as shown in Fig. 1, based on the above idea. The equilibrium condition obtained by the forces acting on a spherical sand grain which are the submerged gravity force W, the sum R_T of the fluid resistance and the resistance resulting from pressure gradient in the downstream direction, the uplift R_L resulting from pressure gradient in the normal direction to the bottom and the resistance R_S resulting from pressure gradient in the direction of the sloping side, as defined in Fig. 1, is expressed as

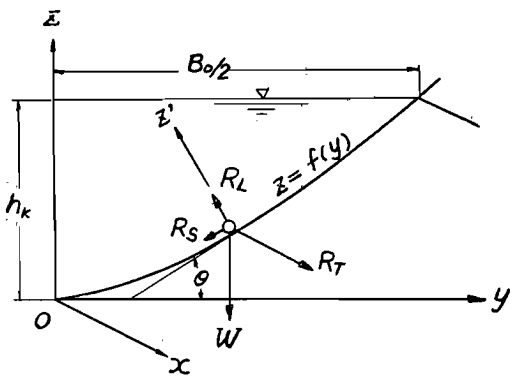

Fig. 1 Definition sketch of the coordinate system and the forces acting on a spherical sand grain on the bottom of the channel having a stable cross section.

$$\{R_T^2+(R_S+W\sin\theta)^2\}^{1/2}=(W\cos\theta-R_L)\tan\varphi,\cdots\cdots\cdots(1)$$

in which φ is the frictional angle of sand grains, and θ the inclination of the sloping side.

Let the diameter of a sand grain be d, the density of water ρ, the density of sand grains σ and the acceleration of gravity g. If the sand grain is assumed to be sphere with a diameter of d, the submerged gravity force W in Eq. (1) is equal to $(\pi/6)d^3(\sigma-\rho)g$. According to the theoretical results on critical tractive force by Iwagaki[10], in Eq. (1), R_L is fairly smaller than R_T, and it is unnecessary to consider R_S except when the inclination of the slop-

ing side becomes extremely large because R_S is also sufficiently smaller than R_T. Therefore, neglecting these forces in Eq. (1) yields

$$\left\{R_T^2+\left\{\frac{\pi}{6}d^3(\sigma-\rho)g\sin\theta\right\}^2\right\}^{1/2}=\frac{\pi}{6}d^3(\sigma-\rho)g\cos\theta\tan\varphi. \quad \cdots\cdots(2)$$

The next problem is how to evaluate the fluid resistance R_T in Eq. (2). The evaluation of this quantity is made by the same method as that used in the previous paper[10]. In the following, the outline of treatment of the fluid resistance will be described.

Considering the laminar sublayer with a thickness of δ_L, as shown in Fig. 2, and denoting the fluid resistance in the part of fully turbulent flow by R_{Tt}, and that in the laminar sublayer by R_{Tl}, the total fluid resistance R_T can be written as

$$R_T=R_{Tt}+R_{Tl}. \quad \cdots\cdots(3)$$

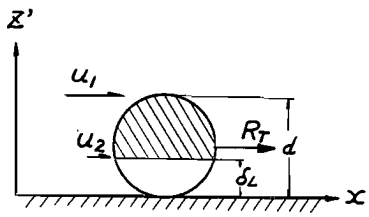

Fig. 2 Schematic drawing of the fluid resistance.

Hence, in Fig. 2, introducing β_s defined by the ratio of the part of fully turbulent flow (area expressed by the shadow) to the projected area of the spherical sand grain, R_{Tt} and R_{Tl} are expressed as

$$R_{Tt}=\frac{\rho}{8}u_1^2C_{D1}\pi d^2\beta_s-\frac{1}{4}\left(\frac{\partial p}{\partial x}\right)_d\pi d^3\beta_s, \quad \cdots\cdots(4)$$

$$R_{Tl}=\frac{\rho}{8}u_2^2C_{D2}\pi d^2(1-\beta_s), \quad \cdots\cdots(5)$$

in which u_1 and u_2 are the velocities in the x-direction at $z'=d$ and $z'=\delta_L$, C_{D1} and C_{D2} are the drag coefficients corresponding to u_1 and u_2, and the second term in Eq. (4) represents the resistance resulting from pressure gradient $\partial p/\partial x$. In evaluating the value of $\partial p/\partial x$, the effect of viscosity is neglected and $-\partial p/\partial x$ is written by $\rho Du/Dt$ based on the Euler's equation of motion. Moreover, introducing the relationships $u=\bar{u}+u'$ and $w=w'$, in which a bar denotes the time-average velocity component and a prime denotes the momentary departure therefrom, and taking an average statistically as Taylor did, the pressure gradient finally becomes

$$-\frac{1}{\rho}\frac{\partial p}{\partial x}=\bar{u}\sqrt{\overline{\left(\frac{\partial u'}{\partial x}\right)^2}}+\sqrt{\overline{u'^2}}\sqrt{\overline{\left(\frac{\partial u'}{\partial x}\right)^2}}+\sqrt{\overline{w'^2}}\frac{d\bar{u}}{dz'}+\sqrt{\overline{w'^2}}\sqrt{\overline{\left(\frac{\partial u'}{\partial z'}\right)^2}}, \quad (6)$$

in which w is the velocity component in the z'-direction.

Since the dimensionless thickness of laminar sublayer $u^*\delta_L/\nu$ changes

with increase in u^*d/ν expressing hydraulic roughness of channel bottom according to Rotta[12], the value of the total fluid resistance R_T is evaluated dividing into three cases in accordance with difference between the size of a sand grain and the thickness of laminar sublayer, in which u^* is the shear velocity on the bottom and ν represents the coefficient of kinematic viscosity.

(1) *The case when* $u^*d/\nu \leq u^*\delta_l/\nu = 6.83$

In this case, the sand grains submerge in the laminar sublayer, and, therefore, R_{Tt} and β_s vanish. Using $u \approx u^*(u^*z'/\nu)$ as the velocity profile in the laminar sublayer, the total fluid resistance can be expressed as

$$R_T = \frac{\rho}{8} u^{*2} C_{D1} \pi d^2 \left(\frac{u^*d}{\nu}\right)^2, \qquad \cdots\cdots\cdots(7)$$

in which the value of the drag coefficient of a sphere in uniform flow corresponding to the following Reynolds number is used for C_{D1}.

$$R_e = \frac{u_1 d}{\nu} = \left(\frac{u^*d}{\nu}\right)^2 \qquad \cdots\cdots\cdots(8)$$

(2) *The case when* $u^*d/\nu \geq 51.1$

The laminar sublayer completely vanishes in this region, so that $R_{Tl} = 0$ and $\beta_s = 1$. Denoting the mixing length by l, the equation of velocity profile is obtained by integrating

$$\frac{d\bar{u}}{dz'} = \frac{u^*}{l} \qquad \cdots\cdots\cdots(9)$$

with the expression for the mixing length suggested by Rotta

$$l = l_0 + 0.4\,z' \qquad \cdots\cdots\cdots(10)$$

and determining the integral constant with the aid of the experimentation of turbulent flow. Since $u^*l_0/\nu \ll u^*d/\nu$ according to Rotta, integration of Eq. (9) gives the following approximate equation for $z \geq d$.

$$\bar{u} = u^*\left(8.5 + 5.75 \log_{10}\frac{z'}{d}\right) \qquad \cdots\cdots\cdots(11)$$

In evaluating the value of pressure gradient expressed by Eq. (6), the minimum scales of eddies, λ_{xx}, $\lambda_{xz'}$ and $\lambda_{z'x}$, and the intensities of turbulence $\sqrt{\overline{u'^2}}$ and $\sqrt{\overline{w'^2}}$ are assumed as

$$\left.\begin{aligned} &\sqrt{\overline{u'^2}} = 2l\frac{d\bar{u}}{dz'} = 2u^*, \quad \sqrt{\overline{w'^2}} = l\frac{d\bar{u}}{dz'} = u^*, \\ &\lambda_{xx} = \sqrt{2}\,\lambda_{xz'} = \sqrt{2}\,\lambda_{z'x} = \sqrt{2}\,(\lambda_0 + 5\,z'). \end{aligned}\right\} \cdots\cdots\cdots(12)$$

Using these relations and Eq. (10), Eq. (6) is finally written as

$$-\frac{1}{\rho}\frac{\partial p}{\partial x}=u^{*2}\left\{\frac{2(8.5+5.75\log z'/d)}{\lambda_0+5z'}+\frac{4}{\lambda_0+5z'}+\frac{1}{l_0+0.4z'}+\frac{2\sqrt{2}}{\lambda_0+5z'}\right\}. \cdots(13)$$

Since u_1 is assumed to be equal to the sum of $\bar{u}$ at $z'=d$ in Eq. (11) and $\sqrt{\overline{u'^2}}$ in Eq. (12), $u_1=(\bar{u}+\sqrt{\overline{u'^2}})_1=10.5\,u^*$. Substituting this relation and $\partial p/\partial x$ at $z'=d$ obtained from Eq. (13) into Eq. (4), the total fluid resistance becomes

$$R_T=\frac{\rho}{8}u^{*2}\pi d^2\left(10.5^2C_{D1}+\frac{47.6}{5+\frac{u^*\lambda_0}{\nu}\Big/\frac{u^*d}{\nu}}+\frac{2}{0.4+\frac{u^*l_0}{\nu}\Big/\frac{u^*d}{\nu}}\right), \cdots(14)$$

in which u^*l_0/ν is obtained from the relation suggested by Rotta[12] as a function of u^*d/ν, and $u^*\lambda_0/\nu$ is assumed to be the same relation as u^*l_0/ν. The Reynolds number necessary to evaluate the value of C_{D1} in Eq. (14) is

$$R_e=\left(\frac{\bar{u}d}{\nu}\right)_1=8.5\frac{u^*d}{\nu}. \quad \cdots\cdots\cdots\cdots(15)$$

(3) *The case when* $6.83\leq u^*d/\nu\leq 51.1$

In this case, since a part of the sand grain is exposed to fully turbulent flow outside the laminar sublayer, both R_{Tt} and R_{Tl} must be considered. Using the following expression for the velocity profile,

$$\frac{d\bar{u}}{dz'}=\frac{\sqrt{4l^2u^{*2}+\nu^2}}{2l^2}-\frac{\nu}{2l^2}, \quad \cdots\cdots\cdots\cdots(16)$$

or

$$\bar{u}=u^*\left\{\frac{1}{0.4\xi}\left(\frac{1}{2}-\sqrt{\xi^2+\frac{1}{4}}\right)+2.5\log_e 2\left(\xi+\sqrt{\xi^2+\frac{1}{4}}\right)+\frac{u^*\delta_L}{\nu}\right\}, \cdots(16)'$$

in which $\xi=u^*l/\nu=0.4(u^*z'/\nu-u^*\delta_L/\nu)$, and calculating the value of $\partial p/\partial x$ at $z'=d$ in the same manner as in the case (2) by using Eqs. (16) and (16)', the total fluid resistance is written as

$$\begin{aligned}R_T=\frac{\rho}{8}u^{*2}\pi d^2\Bigg[&C_{D1}\beta_s\left\{2.5\log_e 2\left(\xi_1+\sqrt{\xi_1^2+\frac{1}{4}}\right)-\frac{1}{4\xi_1}\left(2\sqrt{\xi_1^2+\frac{1}{4}}-1\right)\right.\\&\left.+\frac{u^*\delta_L}{\nu}\right\}^2+2\beta_s\frac{2\sqrt{\xi_1^2+\frac{1}{4}}-1}{\left(1-\frac{u^*\delta_L}{\nu}\Big/\frac{u^*d}{\nu}\right)\xi_1}\left\{\frac{1}{2}\log_e 2\left(\xi_1+\sqrt{\xi_1^2+\frac{1}{4}}\right)\right.\\&-\frac{1}{4\xi_1}\left(2\sqrt{\xi_1^2+\frac{1}{4}}-1\right)+0.2\frac{u^*\delta_L}{\nu}+\frac{(\sqrt{4\xi_1^2+1}-1)}{\xi_1}\left(0.825\right.\\&\left.\left.+\frac{1}{2}\sqrt{\frac{2}{25}+\frac{1}{4\xi_1^2+1}}\right)\right\}+C_{D2}(1-\beta_s)\left(\frac{u^*\delta_L}{\nu}\right)^2\Bigg], \quad \cdots\cdots\cdots\cdots(17)\end{aligned}$$

in which $\xi_1=0.4(u^*d/\nu-u^*\delta_L/\nu)$, and C_{D1} and C_{D2} are the functions of the Reynolds numbers defined by

$$R_{e1}=\frac{\bar{u}_1 d}{\nu}=\frac{u^* d}{\nu}\left\{2.5\log_e(2\xi_1+\sqrt{4\xi_1^2+1})-\frac{1}{0.8\xi_1}(\sqrt{4\xi_1^2+1}-1)+\frac{u^*\delta_L}{\nu}\right\} \quad \cdots\cdots(18)$$

and

$$R_{e2}=\frac{\bar{u}_2 d}{\nu}=\frac{u^* d}{\nu}\frac{u^*\delta_L}{\nu} \quad \cdots\cdots(19)$$

respectively. $u^*\delta_L/\nu$ is a function of u^*d/ν as was disclosed by Rotta, and, therefore, β_s which is related with $\delta_L/d=(u^*\delta_L/\nu)/(u^*d/\nu)$ is also a function of u^*d/ν.

Finally, for all three cases, the fluid resistance is generally expressed as

$$R_T=\frac{\rho}{8}u^{*2}\pi d^2 F\left(\frac{u^*d}{\nu}\right), \quad \cdots\cdots(20)$$

in which F is the distinct function of u^*d/ν only for each case as seen in Eqs. (7), (14) and (17).

Substituting Eq. (20) into Eq. (2), and applying the relation $\cos^2\theta=1/\{1+(dz/dy)^2\}$, the equilibrium condition is written as

$$\left(\frac{dz}{dy}\right)^2=\left[\tan^2\varphi-\left\{\frac{3}{4}\frac{u^{*2}}{(\sigma/\rho-1)gd}F\right\}^2\right]\Big/\left[1+\left\{\frac{3}{4}\frac{u^{*2}}{(\sigma/\rho-1)gd}F\right\}^2\right]. \quad (21)$$

Thus, the dimensionless forms defined by

$$z=h_k\zeta, \qquad y=h_k\eta \quad \cdots\cdots(22)$$

are introduced, and the shear velocity on the channel bottom is assumed to hold the relation expressed by

$$u^{*2}=u_c^{*2}(1-\zeta), \quad \cdots\cdots(23)$$

in which h_k is the maximum depth of the stable channel, and u_c^* denotes the shear velocity corresponding to h_k and the channel slope S. These expressions for z, y and u^* in Eq. (21) yield

$$\frac{d\zeta}{d\eta}=\pm\sqrt{\frac{\tan^2\varphi-K^2(1-\zeta)^2}{1+K^2(1-\zeta)^2}}, \quad \cdots\cdots(24)$$

in which $$K=\frac{3}{4}\frac{u_c^{*2}}{(\sigma/\rho-1)gd}F\left(\frac{u^*d}{\nu}\right).$$

In Eq. (24), $d\zeta/d\eta$ must be zero at $\zeta=0$, i.e. on the bed at the maximum depth, which means that this condition corresponds approximately to the critical tractive force in the case of two-dimensional flow. On the other hand, when $\zeta=1$, the right side of Eq. (24) becomes $\tan\varphi$, which shows that the inclination of the sloping side of the channel equals the frictional angle of sand grains at the edge of water surface.

Eq. (24) has been derived theoretically considering the equilibrium con-

dition for only a sand grain resting on the rough bottom of the channel. However, actually a lot of sand grains are exposed to the flow and shelter each other to some extent, so that the magnitude of the real fluid resistance will be less than that computed above under the assumption that only a sand grain rests on the rough bottom. In order to represent this effect of sheltering, Iwagaki[10] multiplied the theoretical fluid resistance by 0.4 named as the sheltering coefficient. In the present approach, following the same treatment, Eq. (24) is modified as follows.

$$K=\frac{3}{4}\frac{u_c^{*2}}{(\sigma/\rho-1)gd}\varepsilon F\left(\frac{u^*d}{\nu}\right), \qquad \cdots\cdots\cdots\cdots(25)$$

in which ε can be estimated by the condition $d\zeta/d\eta=0$ at $\zeta=0$. Because $u_c^{*2}/(\sigma/\rho-1)gd$ is the function of u_c^*d/ν and $\tan\varphi$[10], it is seen by considering Eq. (23) that the right side of Eq. (24) is the function of u_c^*d/ν, $\tan\varphi$ and ζ. Eventually, F in Eq. (25) is summarized as follows.

For the case when $(u_c^*d/\nu)\sqrt{1-\zeta}\leq 6.83$,

$$F=C_{D1}\left(\frac{u_c^*d}{\nu}\right)^2(1-\zeta). \qquad \cdots\cdots\cdots\cdots(26)$$

For the case when $6.83\leq(u_c^*d/\nu)\sqrt{1-\zeta}\leq 51.1$,

$$\begin{aligned}F=&C_{D1}\beta_s\left\{2.5\log_e(2\xi_1+\sqrt{4\xi_1^2+1})-\frac{1}{4\xi_1}(\sqrt{4\xi_1^2+1}-1)+\frac{u^*\delta_L}{\nu}\right\}^2\\&+\frac{2\beta_s\left(2\sqrt{\xi_1^2+\frac{1}{4}}-1\right)}{\left(1-\frac{u^*\delta_L}{\nu}\Big/\frac{u^*d}{\nu}\right)\xi_1}\left\{\frac{1}{2}\log_e 2\left(\xi_1+\sqrt{\xi_1^2+\frac{1}{4}}\right)-\frac{1}{4\xi_1}\left(2\sqrt{\xi_1^2+\frac{1}{4}}-1\right)\right.\\&\left.+0.2\frac{u^*\delta_L}{\nu}+\frac{(\sqrt{4\xi_1^2+1}-1)}{\xi_1}\left(0.825+\frac{1}{2}\sqrt{\frac{2}{25}+\frac{1}{4\xi_1^2+1}}\right)\right\}\\&+C_{D2}(1-\beta_s)\left(\frac{u^*\delta_L}{\nu}\right)^2. \qquad \cdots\cdots\cdots\cdots(27)\end{aligned}$$

For the case when $(u_c^*d/\nu)\sqrt{1-\zeta}\geq 51.1$,

$$F=10.5^2C_{D1}+\frac{47.6}{5+\frac{u^*\lambda_0}{\nu}\Big/\frac{u^*d}{\nu}}+\frac{2}{0.4+\frac{u^*l_0}{\nu}\Big/\frac{u^*d}{\nu}}. \qquad \cdots\cdots\cdots\cdots(28)$$

The equation given by Eq. (24) with the aid of Eqs. (25), (26), (27) and (28), therefore, represents the fundamental equation of the stable cross section based on the concept that, as already mentioned, all sand grains on the channel bottom are under the critical condition for incipient motion.

2.2 Numerical results and its consideration

Profiles of the stable cross section can be obtained by integrating Eq. (24) numerically under the condition $\zeta=0$ at $\eta=0$. For the sake of calculation, Eq. (24) is written as

$$\eta=\pm\int_0^{\zeta}\sqrt{\frac{1+K^2(1-\zeta)^2}{\tan^2\varphi-K^2(1-\zeta)^2}}d\zeta. \qquad \cdots\cdots\cdots\cdots(29)$$

Since $\tan\varphi$ has approximately constant value 1.0, $u_c{}^{*2}/(\sigma/\rho-1)gd$ is the known function of $u_c{}^*d/\nu$ only[10]. Therefore, under the given values of $u_c{}^*d/\nu$ if the size of sand gravel on the bottom is uniform along the cross section of the channel, the above integration is easily performed by numerical computation. Fig. 3 represents some examples of the profiles of the stable cross section computed for various values of $u_c{}^*d/\nu$ and $\tan\varphi=1$. Variation of the

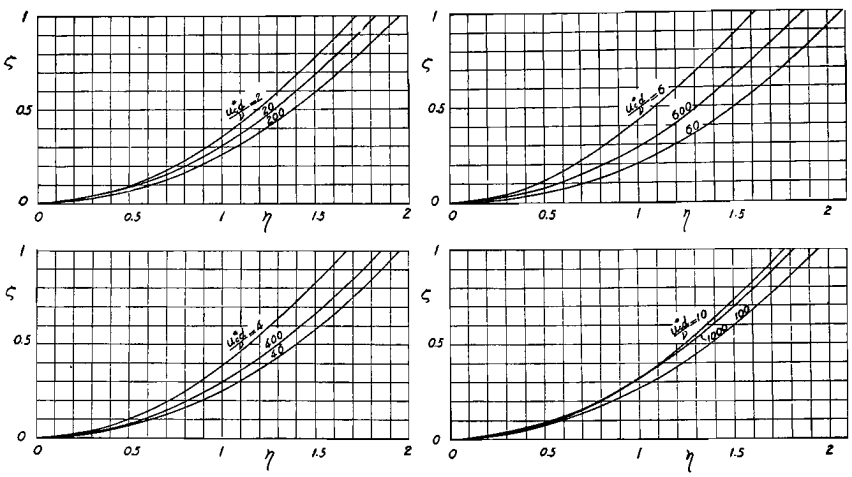

Fig. 3 Some examples of the profiles of the stable cross section.

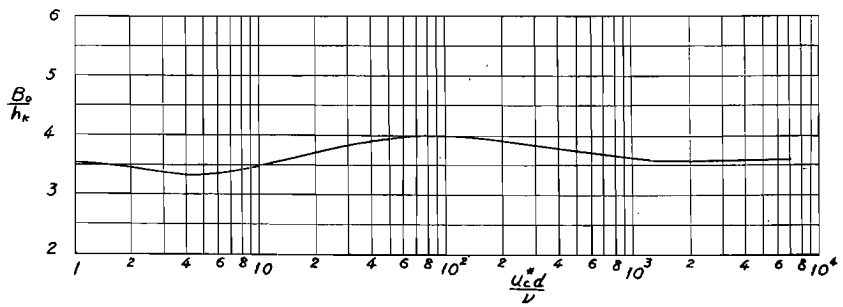

Fig. 4 Variation of the dimensionless width of water surface B_0/h_k with $u_c{}^*d/\nu$.

width of water surface with values of u_c^*d/ν is shown in the dimensionless form B_0/h_k in Fig. 4. The results show that the profiles of the stable cross section obtained by the above dimensionless forms are nearly constant with increase in u_c^*d/ν, except that the width of water surface becomes maximum

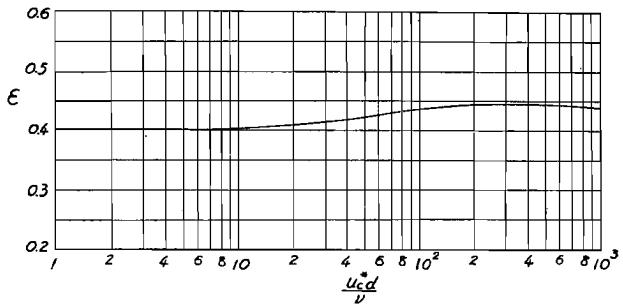

Fig. 5 Variation of the sheltering coefficient ε and u_c^*d/ν.

at $u_c^*d/\nu \approx 70$. Fig. 5 shows the sheltering coefficient as a function of u_c^*d/ν used in the computation, and it indicates that the value of the coefficient is a little larger than 0.4 concluded by Iwagaki because the uplift resulting from velocity fluctuation is, as already described, ignored for the fluid resistance. Moreover, the distribution of the shear velocity as a function of η can be calculated from the numerical results obtained previously and Eq. (23).

3. Experiment

In order to verify Eq. (23) assumed in deriving the equation of the stable cross section, the experiments were conducted. The experimental data of the shear velocity on the fixed bed of the channel having the stable cross section expressed by Eq. (29), were compared with the theoretical results based on Eq. (23). In this case, the shear velocities were obtained indirectly by measuring the velocity profiles.

3.1 Experimental apparatus and procedure

(1) *Experimental channel*

In the rectangular channel with a length of 10.5 m, a width of 20 cm and a depth of 8 cm, the stable cross section obtained by Eq. (29) was made of mortar corresponding to u_c^*d/ν, and the channel bed of mortar was coated

with carefully sieved sand grains. In the channel, an apparatus for measuring the velocity profile in the normal direction to the channel bottom was set at 7.0 m from the upstream end of the channel and that of controlling the back-water effect to the uniform flow at the down stream end. The slope of the channel was accurately adjustable.

(2) *Properties of used sands*

The size of sand grains is necessary to be small by the reason mentioned in (3). Table 1 summarizes the grain diameters, the specific gravities and the frictional angles of used sands.

Table 1 Grain diameters, specific gravities and frictional angles of used sands and u_c^*d/ν.

d cm	σ/ρ	$\tan\varphi$	u_c^*d/ν
0.1435	2.564	0.959	35.0
0.0223	2.530	0.945	2.41

(3) *Measurement of the shear velocity*

The velocity profile for flows in pipes and two-dimensional open channels, when z' is sufficient large, is given by

$$\bar{u} = A_r u^* + 5.75 \log_{10} z'/d, \qquad \cdots\cdots\cdots\cdots(30)$$

in which A_r is generally a function of u^*d/ν and especially constant for the rough boundary as shown in Eq. (11). Under the assumption that Eq. (30) is applicable to the flow close to sand grains on the channel bottom even in this case, the velocity profiles in the normal direction to the channel bottom were measured, and the velocity $\bar{u}$ was plotted against $\log_{10} z'/d$. This relation becomes straight, and therefore, dividing the slope of the straight line by 5.75 the shear velocity u^* is found.

Measurements of velocity profiles were made with the Pitot tube of an outer diameter 1.8 mm for many sections on both sides of the stream channel.

3.2 Experimental results and comparison with the theoretical results

(1) *Experimental results*

Experiments were conducted for two cases $u_c^*d/\nu = 35.0$ and 2.41 determined by the grain diameters and water temperature as shown in Table 1. In each case, by dropping the sand grains in the stream flow, it was examined that the flow at the center of the channel was under the condition of critical tractive force, and also for other locations of the channel bottom the same examinations were performed. The results of the examinations for every location of the bottom were satisfactory. Some typical examples of the measured

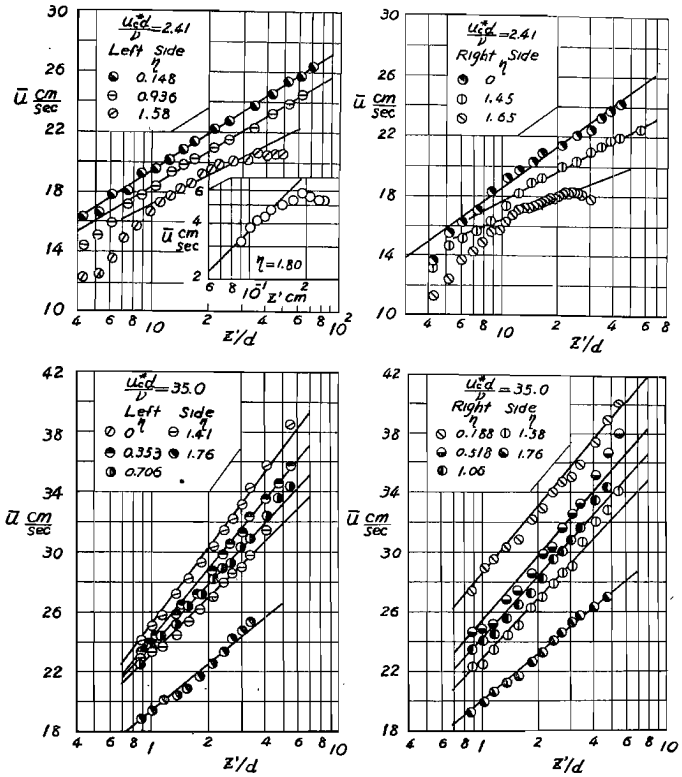

Fig. 6 Some typical examples of the velocity distributions.

velocity distributions are shown in Fig. 6.

In plotting the velocity against $\log_{10} z'/d$, the origin of the coordinate z' should be questioned. Especially, when the grain size is large, the velocity profile is much different by the location of the origin. In this case, the sands with sufficiently small grain diameters were used, and the location of the origin was taken $d/4$ below the top of a sand grain. It is evident from the results shown in Fig. 6 that Eq. (30) can be applied to this case except when θ is large. Thus, u^* and A_r are obtained by the procedure previously described. When u^*d/ν is very small, however, the shear velocity is determined by the relation $u=u^*(u^*z'/\nu)$ for laminar sublayer.

(2) *Comparison with the theoretical results*

The distributions of the measured shear velocity on the channel bottom. which are expressed by the dimensionless forms u^*d/ν and $u^{*2}/(\sigma/\rho-1)gd$,

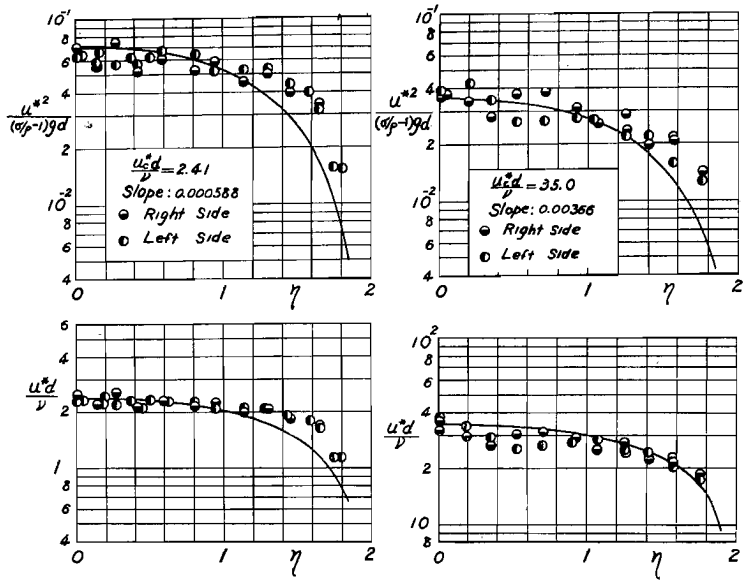

Fig. 7 Comparison of the shear velocity distributions between the experimental results and the theoretical curves.

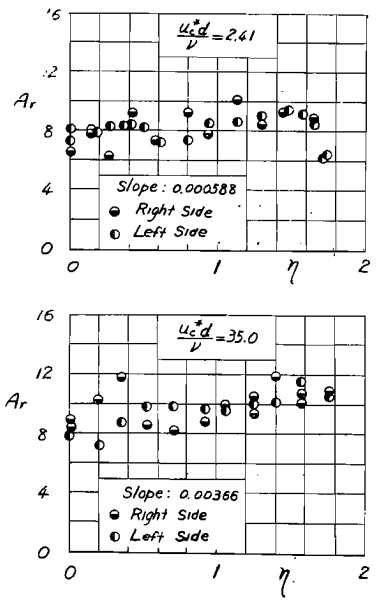

Fig. 8 Variations of A_r with η.

are shown in Fig. 7 with the theoretical curves for $u_c^* d/\nu = 2.41$ and 35.0. It is seen from Fig. 7 that the theoretical curves agree well with the experimental results except for large values of η though the data plotted are scattering. The trend that near the edge of water surface the plotted data are a little larger than the theoretical values, will be evidently due to the reason that the flow near the edge of water surface cannot be sufficiently approximate to the two-dimensional flow because of increase in the inclination of the sloping side, and, in addition, there the water depth increases locally by the capillary effect. Fig. 8 shows the variations of A_r with η. Most of the data for $u_c^* d/\nu = 2.41$

and 35.0 belong to the regions of the hydraulically smooth boundary and transitional boundary respectively.

4. Some Fundamental Data to Design Problems

In the United States of America, the design of canals and channels with erodible material has usually been approached from the standpoint of the regime method, but recently studies using the tractive force criteria have been made. In Europe, the tractive force criteria has sometimes been used. In this chapter, therefore, some fundamental data required in designing the stable channel with the cross section obtained in Chapter 2, are described in order to contribute to design practice.

4.1 Depth at the center of the channel

In designing the stable channel, in advance, the size of sand gravel or the slope of the channel bed must be determined. If the size of sand gravel is given, the critical tractive force corresponding to it, is computed by Iwagaki's formula as follows[10].

$$\left.\begin{aligned} R^*\geq 671\,;\quad & u_c^{*2}=0.05\,(\sigma/\rho-1)gd,\\ 162.7\leq R^*\leq 671\,;\quad & =\{0.01505g(\sigma/\rho-1)\}^{25/22}\nu^{-3/11}d^{31/22},\\ 54.2\leq R^*\leq 162.7\,;\quad & =0.034\,(\sigma/\rho-1)gd,\\ 2.14\leq R^*\leq 54.2\,;\quad & =\{0.1235g(\sigma/\rho-1)\}^{25/32}\nu^{7/16}d^{11/32},\\ R^*\leq 2.14\,;\quad & =0.14\,(\sigma/\rho-1)gd, \end{aligned}\right\}\quad\cdots(31)$$

in which $R^*=(\sigma/\rho-1)^{1/2}g^{1/2}d^{3/2}/\nu$.

As already described, in the present approach, the water depth at the center of a channel h_k was assumed to be closely equal to the depth corresponding to the critical tractive force in two-dimensional flow. The relation between the depth at the center of the channel and the channel slope with a parameter of the grain diameter, based on Eq. (31) with $\sigma/\rho=2.65$, $\nu=0.01$ cm^2/sec (20.3°C) and $g=980$ cm/sec^2, is shown in Fig. 9.

4.2 Some characteristics of the stable cross section

The width of the stable channel, which is one of the characteristics, has been shown in Fig. 4. In the following, the area and the hydraulic radius of the cross section are described.

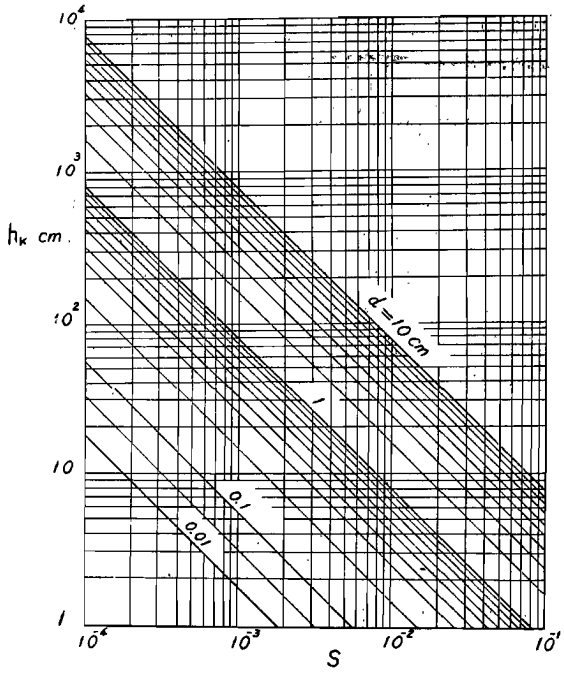

Fig. 9 Relation between the depth of water at the center of the channel and the channel slope with a parameter of the grain diameter.

Considering the general shape of the stable cross section as shown in Fig. 10, the cross-sectional area can be expressed as

$$\frac{A}{h_k^2}=\frac{A_0}{h_k^2}+\frac{B}{h_k}, \quad \cdots\cdots\cdots\cdots(32)$$

in which A is the cross-sectional area, B the width of the bed and A_0 the cross-sectional area when $B=0$. In Eq. (32), A_0/h_k^2 is a function of u_c^*d/ν as shown in Fig. 11.

On the other hand, the hydraulic radius R can be expressed as

$$\frac{R}{h_k}=1-\frac{a}{b+B/2h_k}, \quad \cdots(33)$$

in which a and b are parameters which are the functions of u_c^*d/ν as shown in Fig. 12.

If the mean velocity U is given by

$$U=CR^mS^n, \quad \cdots\cdots\cdots(34)$$

the discharge Q is computed by

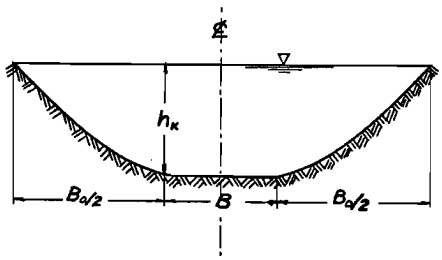

Fig. 10 General shape of the stable cross section.

$$Q=Ch_k^{2+m}S^n\left(\frac{A_0}{h_k^2}+\frac{B}{h_k}\right)\left(1-\frac{a}{b+B/2h_k}\right)^m \quad \cdots\cdots\cdots(35)$$

which is derived by using Eqs. (32), (33) and (34). The discharge coefficient C and the exponents m and n in Eqs. (34) and (35) will be generally functions of the grain diameter d as suggested by Liu and Hwang[18].

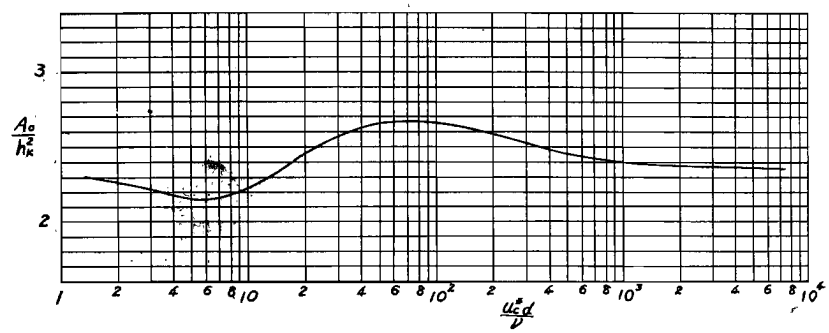

Fig. 11 Variation of the dimensionless cross-sectional area when $B=0$ with $u_c^* d/\nu$.

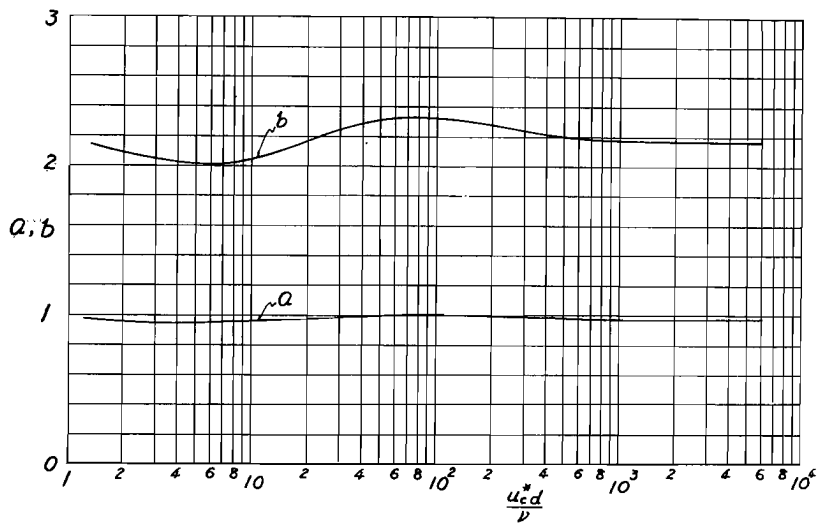

Fig. 12 Variations of the parameters a and b with $u_c^* d/\nu$.

5. Applications of the Theory to the Existing Irrigation Canals

It this chapter, the applications of the theoretical results previously obtained to design problems of irrigation canals are considered by using the existing canal data in Simons' paper[6] and Lane and others' paper[1].

5.1 Distribution of shear velocity

Simons and Bender observed the velocity profiles of twenty four canals and calculated the shear velocity by applying the logarithmic law of velocity distribution. In the present paper, recomputed data of shear velocity by the authors based on the velocity distributions near to the bottom of the canals are used. Fig. 13 represents the comparison of the shear velocities computed from the observed velocity distributions for some of the canals and the estimated shear velocities by Eq. (23). Although the data plotted are much scattering, it may be seen that the relation of Eq. (23) is applicable to the present approach.

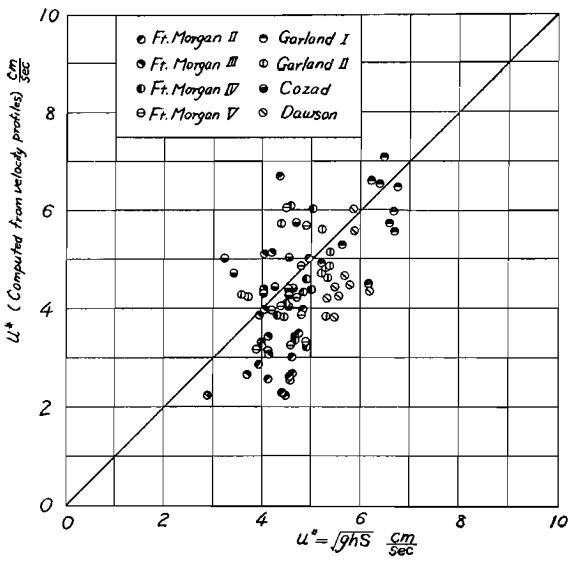

Fig. 13 Comparison of computed shear velocities from observed velocity distributions and estimated shear velocities by Eq. (23).

5.2 Cross sections of the canals

In treating existing canals, the existence of sediment load including wash load must be considered. However, at the present time, the hydraulic analysis of the cross section of such a canal is generally difficult. Although the canals of which the data were taken by Simons and Bender transport suspended load, more or less, the theoretical results are applied to their data below.

The cross sections of twenty four canals are shown in Figs. 14, 15 and 16, in which, as an abscissa, the ratio η' of the distance from the edge of water surface to the depth of water at the center of the canal is taken instead of η in Fig. 3. In order to compare these observed data with the theoretical shapes of the cross sections in Fig. 3, the values of $u_c{}^*d/\nu$ must be determined. Since the canals transport suspended load, the shear velocity has been computed by using the observed depth of water and the observed

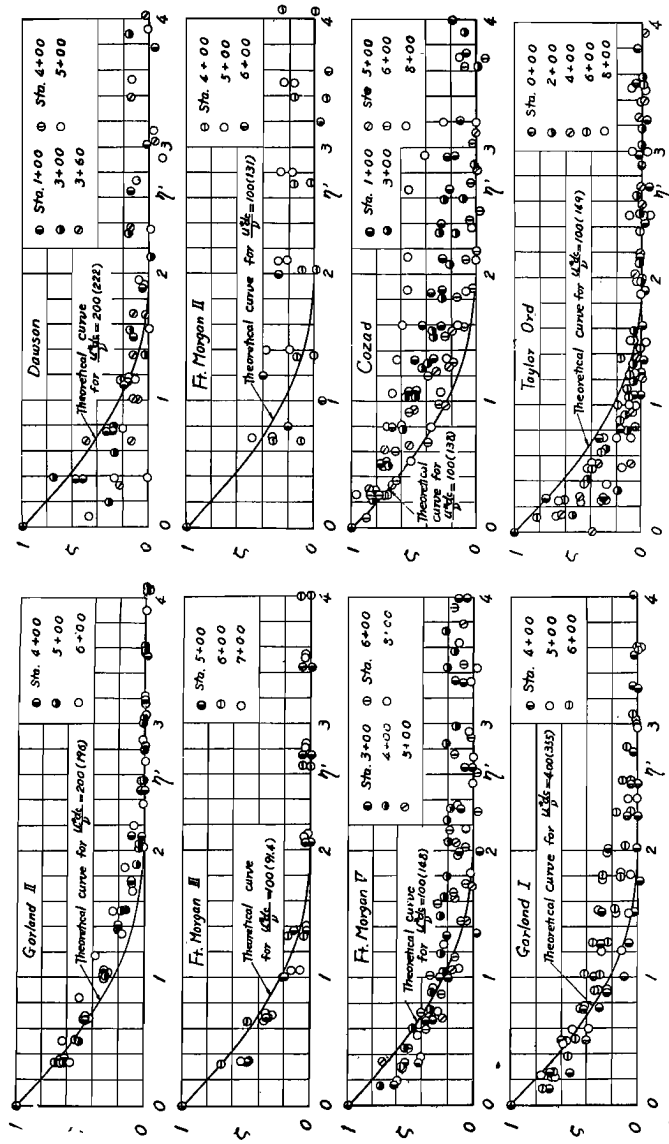

Fig. 14 Cross sections of the canals with non-cohesive materials.

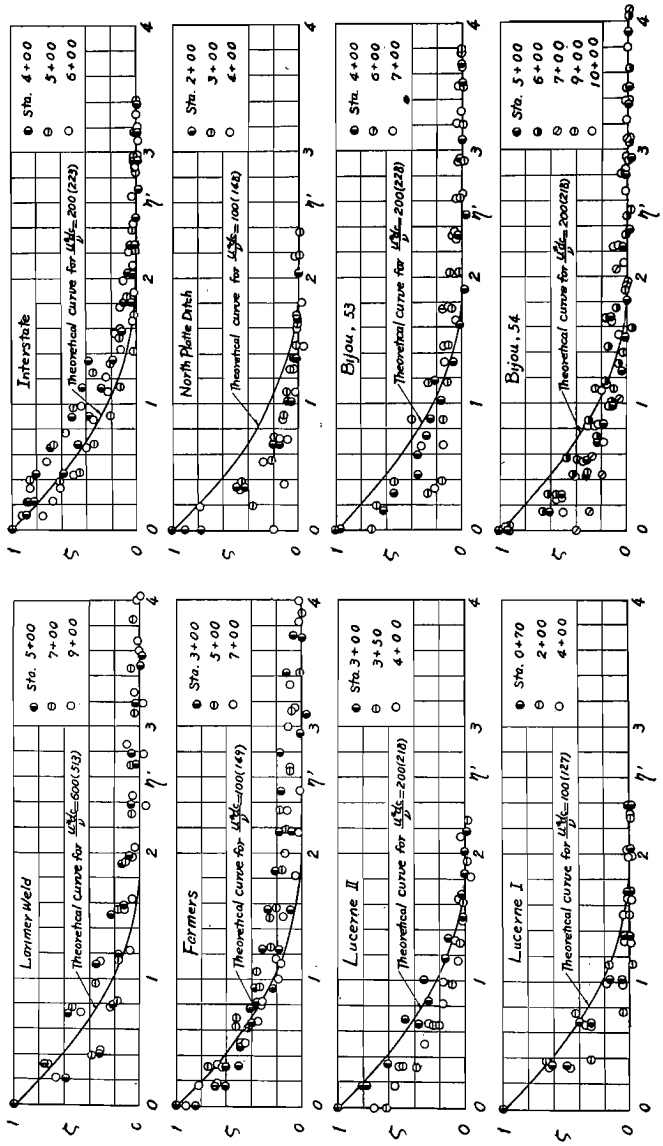

Fig. 15 Cross sections of the canals with moderately cohesive materials.

slope of water surface, and the size of sand grains has been obtained from Eq. (31) by using the observed depth and slope, too. Therefore, the parameter u^*d_c/ν is used instead of u_c^*d/ν. The correlation between d_c and the size of the canal material is discussed in the following section. The theoretical curves in Figs. 14, 15 and 16 are for the values of u_c^*d/ν shown in Fig. 3 close to the values of u^*d_c/ν in the brackets. Figs. 14, 15 and 16 represent the comparisons with the cross sections of the canals with non-cohesive materials, moderately cohesive materials and cohesive materials respectively.

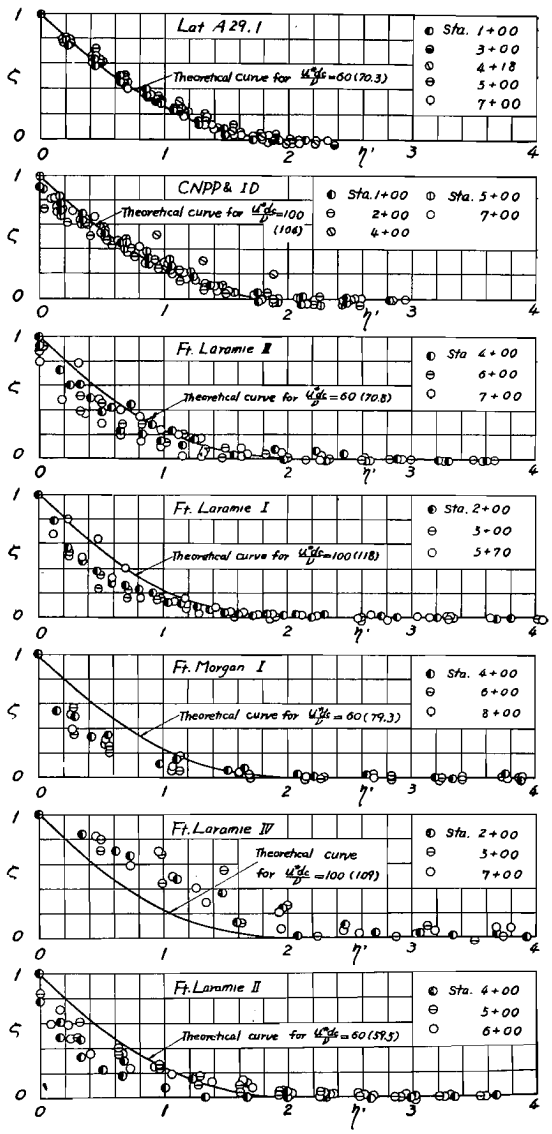

Fig. 16 Cross sections of the canals with cohesive materials.

As is seen in these figures, the agreement of the theoretical shapes with the canal data is fairly good except a few canals, in spite of the theory based on the concept that all sand grains on the bottom of a canal are under the condition of incipient motion. It is found that some of the canals with cohesive and moderately cohesive materials have almost vertical cross sections at the edge of water surface due to the cohesive

effect and the existence of vegetables. Moreover, one of the reasons why the plotted data are much scattering is an asymmetry of the cross section at the right and the left sides of the canals due to probably local secondary currents, non-uniformity of bottom material and others. Conclusively speaking, the essential difference of the stable cross sections between the canals with non-cohesive, moderately cohesive and cohesive materials cannot be found from Figs. 14, 15 and 16.

5.3 Size of canal material

In applying the theoretical results of stable cross sections to the existing canal data, the computed sizes of sand grains d_c for the observed depths of water and slopes have been used in the previous section. Therefore, the correlation between d_c and the size of material constituting the canal is required in design. It will be found by using the regime method.

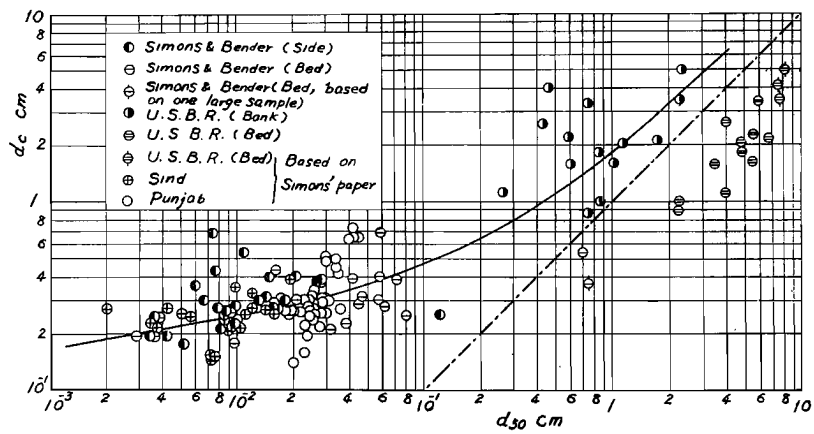

Fig. 17 Relation between computed diameter of sand grains d_c and observed median diameter of side and bed materials d_{50}.

Fig. 17 shows the relation between d_c and the observed median diameter of material d_{50} based on the canal data of Simons & Bender, Punjab, Sind and U.S.B.R. The full line in the figure shows the relation for design, and the chain line indicates the relation $d_c = d_{50}$. It is supposed from the sampling method that the side and bed materials sampled by Simons and Bender will be the materials of the canal banks, nor the materials forming the surface

layer of the canal bed, so that their data will correspond to those of the canal bank of U.S.B.R. It is noted that U.S.B.R. data of the canal bed are not in agreement with the full line and plotted below the chain line. This reason may be explained as follows.

The Rio Grande Canal and the Farmers Union and Prairie Canals, of which U.S.B.R. data were taken, were constructed in 1879 and 1887 respectively[1]. Therefore, the change of the past bed material exposed by excavation into the present bed material for a long time must be taken into account. Lane and others mentioned that most of the canals and laterals are very stable, the original dimensions are not available, and that it is not known to what extent their shape has been modified by the flowing water or by cleaning operations since they were constructed. It is presumed from this fact that the present bed material is not moved by the flowing water any more, because the fine sand grains were transported downstream for a long time, and the stable cross section of the canal has been formed. In order to verify this presumption, Fig. 18 is presented, which shows the relation between the median size of bed material and the median size of bank material larger than the size computed from Eq. (31). It is seen from the figure that both observed (former) and estimated (latter) sizes are approximately same; therefore, the above presumption will be right.

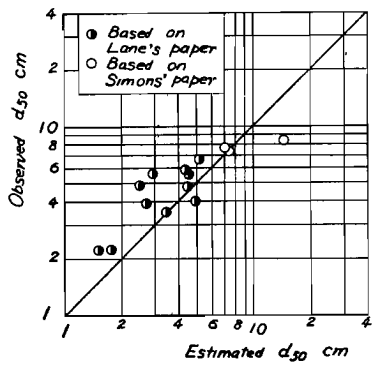

Fig. 18 Relation between observed median diameter of bed material and estimated median diameter of bank material larger than d_c for U.S.B.R. data.

It is summarized that there are two different standpoints in designing the stable cross section of a canal; one is for the canal of which the side stability is good enough in spite of the existence of sediment transport near the center of the canal, and the other is for the canal in which there exists no sediment transport at the final stage. When a canal is designed based on the former standpoint, the value of d_c required first can be estimated from the full line in Fig. 17 for a given canal material, so that the stable cross section for given discharge and slope can be determined by applying the fundamental data to design problems described in Chapter 4. On the other hand, when the latter standpoint is adopted, the value of d_c corresponding to h_k obtained from the

fundamental data in Chapter 4 for given discharge, slope and width of bed is decided, in which the width of bed to give should be estimated considering how many percent of the canal material has sand and gravel larger than d_c, because if the width of bed is estimated too small, d_c becomes large, and, therefore, the final stage of no sediment transport can not be reached.

6. Conclusion

Although the problems of the stable channel have so fruitfully been discussed by many authorities to contribute to designing canals and channels, especially in the United States of America, the hydraulic treatment of the stable cross section of canals has scarcely been conducted due to the very complicated phenomena. The development of the study, therefore, has greatly been desired in irrigation and river projects.

In the present paper, a theoretical approach to the problem of the stable cross section based on the criteria of tractive force has been presented with the experiment to verify the assumption introduced in the theory. The theoretical shapes of the stable cross section have been obtained in the dimensionless form. The comparisons made between the theoretical shapes of the stable cross section and those of twenty four canals of which the data were taken by Simons and Bender in the United States of America are in good agreement. The relation between the median diameters of side and bed materials of many canals in the United States of America and the diameters of sand grains computed from the formula of critical tractive force for depths of water and slopes observed in the canals has been found empirically.

Acknowledgments

The authors wish to express their grateful appreciations to Professor Tojiro Ishihara, Kyoto University, for his constant encouragement to this study and Dr. D. B. Simons, Colorado State University in U.S.A., for his valuable suggestion regarding the application of theory to the existing canals. The present study is a part of the authors' studies supported by the Science Research Expense of the Ministry of Education and thanks are due to the Ministry of Education.

References

1) Carter, A. C., Carlson, E. J. and Lane, E. W. : Critical Tractive Force on

Channel Side Slope, U. S. Bureau of Reclamation Hyd. Lab. Report, No. Hyd-366, 1953, pp. 1-6.
2) Lane, E. W. and Carlson, E. J. : Some Factors Affecting the Stability of Canals Constructed in Course Granular Materials, Proc. Minnesota Int. Hyd. Conv., I. A. H.R., 1953, pp. 37-48.
3) Lane, E. W. : Design of Stable Channels, Trans. A.S.C.E., Vol. 120, 1955, pp. 1234-1279.
4) Terrell, P. W. and Borland, W. M. : Design of Stable Canals and Channels in Erodible Material, Proc. A.S.C.E., Vol. 82, Hyd. Div., Feb. 1956, pp. 1-17.
5) Laursen, E. M. : The Application of Sediment-Transportation Mechanics to Stable-Channel Design, Proc. A.S.C.E., Vol. 82, Hyd. Div., August 1956, pp. 1-11.
6) Simons, D. B. : Theory and Design of Stable Channels in Alluvial Materials, Department of Civil Engineering, Colorado State University, Fort Collins, Colorado, May 1957.
7) Shields, A. : Anwendung der Ähnlichkeitsmechanik und der Turbulenzforschung auf die Geschiebebewegung, Mitteilung der Preussischen Versuchsanstalt für Wasserbau und Schiffbau, Heft 26. Berlin, 1936.
8) White, C. M. : The Equilibrium of Grains on the Bed of a Stream, Proc. Roy. Soc., A 174, 1940, pp. 322-334.
9) Kurihara, M. On the Critical Tractive Force, Reports of the Research Institute for Hydraulic Engineering, Kyushu University, Vol. 4, No. 3, 1948, pp. 1-26 (in Japanese).
10) Iwagaki, Y. : Hydrodynamical Study on Critical Tractive Force, Trans. J.S.C.E., No. 41, 1956, pp. 1-21 (in Japanese).
11) Iwagaki, Y. and Tsuchiya, Y. · On the Critical Tractive Force for Gravels on a Granular Bed in Turbulent Stream, Trans. J.S.C.E., No. 41, 1956, pp. 22-38 (in Japanese).
12) Rotta, J.: Das in Wandnähe gültige Geschwindigkeitsgesetz turbulenter Strömungen, Ingenieur-Archiv, 18 Band, 1950, pp. 277-280.
13) Liu, H. K. and Hwang, S. Y. : A Discharge Formula for Flow in Straight Alluvial Channels, Presented at the meeting of A.S.C.E. in Portland, Oregon, June 1958.

Notation

A = cross-sectional area;
A_0 = cross-sectional area when $B=0$;
A_r = constant in logarithmic law of velocity distribution;
a, b = parameters in Eq. (33);
B = width of bed;
B_0 = width of water surface when $B=0$;
C = discharge coefficient;
C_{D1}, C_{D2} = drag coefficients;
d = diameter of spherical sand grain;

d_c = diameter of sand grain being under critical condition for movement;

F = function of u^*d/ν in Eq. (25);

g = acceleration of gravity;

h_k = depth at center of channel;

K = parameter expressed by Eq. (25);

l, l_0 = mixing lengths;

m, n = empirical exponents in Eq. (34);

p = pressure;

Q = discharge;

R = hydraulic radius;

R^* = dimensionless parameter in Eq. (31);

R_e, R_{e1}, R_{e2} = Reynolds numbers;

R_L = uplift resulting from pressure gradient in normal direction to bottom;

R_S = resistance resulting from pressure gradient in direction of sloping side;

R_T = sum of fluid resistance and resistance resulting from pressure gradient in downstream direction;

R_{Tl} = fluid resistance in laminar sublayer;

R_{Tt} = fluid resistance in part of fully turbulent flow;

S = channel slope;

u = velocity component in x-direction;

$\bar{u}$ = time-average velocity component;

u^* = shear velocity on bottom;

u_c^* = critical shear velocity on bottom;

u_1 = velocity component at $z' = d$;

u_2 = velocity component at $z' = \delta_L$;

u', w' = momentary departures from time-average velocity components;

W = submerged gravity force of sand grain;

w = velocity component in z'-direction;

x, y, z = coordinate axises;

z' = coordinate in normal direction to bottom;

β_s = ratio of part of fully turbulent flow to projected area of sand grain;

δ_L = thickness of laminar sublayer;

ε = sheltering coefficient;

ζ = dimensionless depth of water for stable cross section = z/h_k;

η = dimensionless distance from center of channel = y/h_k;

η' = dimensionless distance from edge of water surface;

θ = inclination of sloping side of channel;

λ_{xx}, $\lambda_{xz'}$, $\lambda_{z'x}$, λ_0 = minimum scales of eddies;

ν = kinematic viscosity;

$\xi = u^*l/\nu = 0.4\,(u^*z'/\nu - u^*\delta_L/\nu)$;

$\xi_1 = 0.4\,(u^*d/\nu - u^*\delta_L/\nu)$;

ρ = density of water;

σ = density of sand grain; and

φ = frictional angle of sand grains.

Publications of the Disaster Prevention Research Institute

The Disaster Prevention Research Institute publishes reports of the research results in the form of bulletins. Publications not out of print may be obtained free of charge upon request to the Director, Disaster Prevention Research Institute, Kyoto University, Kyoto, Japan.

Bulletins :

No. 1 On the Propagation of Flood Waves by Shoitiro Hayami, 1951.
No. 2 On the Effect of Sand Storm in Controlling the Mouth of the Kiku River by Tojiro Ishihara and Yuichi Iwagaki, 1952.
No. 3 Observation of Tidal Strain of the Earth (Part I) by Kenzo Sassa, Izuo Ozawa and Soji Yoshikawa. And Observation of Tidal Strain of the Earth by the Extensometer (Part II) by Izuo Ozawa, 1952.
No. 4 Earthquake Damages and Elastic Properties of the Ground by Ryo Tanabashi and Hatsuo Ishizaki, 1953.
No. 5 Some Studies on Beach Erosions by Shoitiro Hayami, Tojiro Ishihara and Yuichi Iwagaki, 1953.
No. 6 Study on Some Phenomena Foretelling the Occurrence of Destructive Earthquakes by Eiichi Nishimura, 1953.
No. 7 Vibration Problems of Skyscraper. Destructive Element of Seismic Waves for Structures by Ryo Tanabashi, Takuzi Kobori and Kiyoshi Kaneta, 1954.
No. 8 Studies on the Failure and the Settlement of Foundations by Sakurō Murayama, 1954.
No. 9 Experimental Studies on Meteorological Tsunamis Traveling up the Rivers and Canals in Osaka City by Shoitiro Hayami, Katsumasa Yano, Shohei Adachi and Hideaki Kunishi, 1955.
No.10 Fundamental Studies on the Runoff Analysis by Characteristics by Yuichi Iwagaki, 1955.
No.11 Fundamental Considerations on the Earthquake Resistant Properties of the Earth Dam by Motohiro Hatanaka, 1955.
No.12 The Effect of the Moisture Content on the Strength of an Alluvial Clay by Sakurō Murayama, Kōichi Akai and Tōru Shibata, 1955.
No.13 On Phenomena Forerunning Earthquakes by Kenzo Sassa and Eiichi Nishimura, 1956.
No.14 A Theoretical Study on Differential Settlements of Structures by Yoshitsura Yokoo and Kunio Yamagata, 1956.
No.15 Study on Elastic Strain of the Ground in Earth Tides by Izuo Ozawa, 1957.
No.16 Consideration on the Mechanism of Structural Cracking of Reinforced Concrete Buildings Due to Concrete Shrinkage by Yoshitsura Yokoo and S. Tsunoda. 1957.
No.17 On the Stress Analysis and the Stability Computation of Earth Embankments by Kōichi Akai, 1957.
No.18 On the Numerical Solutions of Harmonic, Biharmonic and Similar Equations by the Difference Method Not through Successive Approximations by Hatsuo Ishizaki, 1957.
No.19 On the Application of the Unit Hydrograph Method to Runoff Analysis for Rivers in Japan by Tojiro Ishihara and Akiharu Kanamaru, 1958.
No.20 Analysis of Statically Indeterminate Structures in the Ultimate State by Ryo Tanabashi, 1958.
No.21 The Propagation of Waves near Explosion and Fracture of Rock (I) by Soji Yoshikawa, 1958.
No.22 On the Second Volcanic Micro-Tremor at the Volcano Aso by Michiyasu Shima, 1958.
No.23 On the Observation of the Crustal Deformation and Meteorological Effect on It at Ide Observatory and on the Crustal Deformation Due to Full Water and Accumulating Sand in the Sabo-Dam by Michio Takada, 1958.
No.24 On the Character of Seepage Water and Their Effect on the Stability of Earth Embankments by Kōichi Akai, 1958.
No.25 On the Thermoelasticity in the Semi-infinite Elastic Soid by Michiyasu Shima
No.26 On the Rheological Characters of Clay (Part 1) by Sakurō Murayama and Tōru Shibata, 1958.
No.27 On the Observing Instuments and Tele-metrical Devices of Extensometers and Tiltmeters at Ide Observatory and On the Crustal Strain Accompanied by a Great Earthquake by Michio Takada, 1958.
No. 28 On the Sensitivity of Clay by Shinichi Yamaguchi, 1959.
No.29 An Analysis of the Stable Cross Section of a Stream Channel by Yuichi Iwagaki and Yoshito Tsuchiya, 1959.

Bulletin No. 29 Published March, 1959

昭和 34 年 3 月 20 日 印 刷
昭和 34 年 3 月 25 日 発 行
編輯兼発行者 京都大学防災研究所
印刷者 山 代 多 三 郎
京都市上京区寺之内通小川西入
印刷所 山代印刷株式会社